

Dynamic Range Reduction via Branch-and-Bound

Thore Gerlach¹, Nico Piatkowski¹

¹Fraunhofer IAIS

Sankt Augustin 53757, Germany
thore.gerlach@iais.fraunhofer.de

Abstract

The demand for high-performance computing in machine learning and artificial intelligence has led to the development of specialized hardware accelerators like Tensor Processing Units (TPUs), Graphics Processing Units (GPUs), and Field-Programmable Gate Arrays (FPGAs). A key strategy to enhance these accelerators is the reduction of precision in arithmetic operations, which increases processing speed and lowers latency—crucial for real-time AI applications. Precision reduction minimizes memory bandwidth requirements and energy consumption, essential for large-scale and mobile deployments, and increases throughput by enabling more parallel operations per cycle, maximizing hardware resource utilization. This strategy is equally vital for solving NP-hard quadratic unconstrained binary optimization (QUBO) problems common in machine learning, which often require high precision for accurate representation. Special hardware solvers, such as quantum annealers, benefit significantly from precision reduction. This paper introduces a fully principled Branch-and-Bound algorithm for reducing precision needs in QUBO problems by utilizing dynamic range as a measure of complexity. Experiments validate our algorithm’s effectiveness on an actual quantum annealer.

1 Introduction

Hardware acceleration is a major driving force in the recent advent of artificial intelligence (AI). Virtually all large-scale AI models rely on hardware accelerated training via Tensor Processing Units (TPUs), Graphics Processing Units (GPUs), or Field-Programmable Gate Arrays (FPGAs). A key ingredient of these accelerators is parallelism—a large computation is split into smaller pieces, solved via multiple compute units. Clearly, each compute unit must read its inputs from memory. However, memory bandwidth is limited. Hence, to achieve a large level of parallelism, the input that each compute unit needs must be as small as possible. To this end, model parameters with limited precision, e.g., 16-bit, 8-bit, or even smaller, are considered and special training procedures are employed to directly train models with low-precision parameters (Choukroun et al. 2019).

AI accelerators usually rely on parallel implementations of basic linear algebra routines. There is, however, a mul-

titude of AI problems whose inherent computational complexity does not stem from linear algebra operations. Examples include clustering (Aloise et al. 2009), probabilistic inference (Ermon et al. 2013), or feature selection (Brown 2009). At the core of these tasks lies a combinatorial optimization (CO) problem. As of today, solving such CO problems in AI is out of reach for high-dimensional instances. However, analog devices (Yamamoto et al. 2020; Mohseni, McMahon, and Byrnes 2022; Mastiyage Don et al. 2023), ASICs (Matsubara et al. 2020), FPGAs (Mücke, Piatkowski, and Morik 2019; Kagawa et al. 2020), and quantum computers (Albash and Lidar 2018) have recently made promising progress when it comes to solving CO problems.

In particular, we consider Quadratic Unconstrained Binary Optimization (QUBO) (Punnen 2022) problems

$$\min_z z^T Q z, \quad (1)$$

where Q is real and z is binary (proper definitions follow in Section 2). Despite problem (1)’s simple structure, it is NP-hard, and hence covers a plethora of real-world optimization challenges, from problems like the traveling salesperson and graph coloring (Lucas 2014) to machine learning (ML) (Baukhage et al. 2018; Mücke et al. 2023) and various other applications, e.g., (Biesner et al. 2022; Chai et al. 2023).

One common issue of QUBO hardware solvers is limited physical precision of the matrix entries, as real-world hardware devices use finite numerical representations. It turns out that simply truncating decimal digits of Q is not sufficient, since the resulting optimization problem will have different local and global optima (Mücke, Gerlach, and Piatkowski 2023). Hence, truncation renders the resulting optimization problem useless. In the paper at hand, we develop an algorithmic machinery for reducing the numeric precision required to represent a AI-related QUBO instances.

We consider the dynamic range (DR) of any QUBO matrix as a measure of complexity. We present a novel iterative procedure, which reduces the DR while preserving the optimal solution of the underlying QUBO problem. We explain why greedy methods are likely to produce sub-optimal results and propose a novel method that is based on policy roll-out (Bertsekas, Tsitsiklis, and Wu 1997; Silver et al. 2016) to address the greedy nature of baseline methods.

Our contributions can be summarized as follow:

- We formulate the problem of reducing the required numeric precision via a Markov decision process and introduce a fully principled Branch-and-Bound algorithm for exactly solving the problem in a finite number of steps.
- We propose effective and efficiently computable bounds for drastically pruning the search space size.
- Combining our algorithm with the well-known rollout policy, we further improve efficiency and performance.
- We support our theoretical insights with an experimental analysis on AI-related problems and actual quantum hardware. The results show the effectiveness of our precision reduction and the superiority over baselines.

2 Background

We denote matrices with bold capital letters (e.g. \mathbf{A}) and vectors with bold lowercase letters (e.g. \mathbf{a}). Sets will be symbolized by calligraphical or blackboard bold capital letters (e.g. \mathcal{A} , \mathbb{A}). Let the index set from 1 to n be denoted as $[n] := \{1, \dots, n\}$. For an optimization problem, something optimal will be denoted by the superscript “ $*$ ”. We use “ $\hat{}$ ” or “ $\check{}$ ” to indicate a maximum/upper bound or a minimum/lower bound, respectively.

2.1 QUBO

A QUBO problem is completely characterized by an upper triangular matrix $\mathbf{Q} \in \mathbb{R}^{n \times n}$. The QUBO energy of a binary vector $\mathbf{z} \in \{0, 1\}^n$ is defined as

$$E_{\mathbf{Q}}(\mathbf{z}) := \mathbf{z}^{\top} \mathbf{Q} \mathbf{z} = \sum_{i \leq j} Q_{ij} z_i z_j. \quad (2)$$

The objective of a QUBO problem is to find a binary vector $\mathbf{z}^* \in \{0, 1\}^n$ which optimizes the QUBO energy

$$\mathbf{z}^* \in \mathcal{Z}^*(\mathbf{Q}) := \arg \min_{\mathbf{z} \in \{0, 1\}^n} E_{\mathbf{Q}}, \quad (3)$$

where $\mathcal{Z}^*(\mathbf{Q})$ is the set of optimizers for the QUBO problem with matrix \mathbf{Q} . Let \mathcal{Q}_n denote the set of upper triangular matrices in $\mathbb{R}^{n \times n}$. The problem in Eq. (3) is NP-hard (Pardalos and Jha 1992), i.e., in the worst case, the best known algorithm is an exhaustive search over an exponentially large candidate space. Furthermore, any problem in NP can be reduced to QUBO with only polynomial overhead, making this formulation a very general form for combinatorial optimization. A range of solution techniques has been developed over past decades, e.g., exact methods (Narendra and Fukunaga 1977; Rehfeldt, Koch, and Shinano 2023) with worst-case exponential running time, approximate techniques such as simulated annealing (Kirkpatrick, Gelatt Jr, and Vecchi 1983), tabu search (Glover and Laguna 1998), and genetic programming (Goldberg and Kuo 1987); see (Kochenberger et al. 2014) for a comprehensive overview.

2.2 Dynamic Range

Although the entries of a QUBO matrix are theoretically real-valued, real-world computing devices have limits on the precision with which numbers can be represented.

To quantify the precision required to accurately represent QUBO parameters, we adopt the concept of dynamic range

(DR) from signal processing. For this, we first define the set absolute differences between all elements of $\mathcal{X} \subset \mathbb{R}$ as $\mathcal{D}(\mathcal{X}) := \{|x - y| : x, y \in \mathcal{X}, x \neq y\}$, and write $\hat{\mathcal{D}}(\mathcal{X}) := \min \mathcal{D}(\mathcal{X})$ and $\check{\mathcal{D}}(\mathcal{X}) := \max \mathcal{D}(\mathcal{X})$. For a given QUBO matrix $\mathbf{Q} \in \mathcal{Q}_n$ the DR is defined as

$$\text{DR}(\mathbf{Q}) := \log_2 \left(\frac{\hat{\mathcal{D}}(\mathcal{U}(\mathbf{Q}))}{\check{\mathcal{D}}(\mathcal{U}(\mathbf{Q}))} \right), \quad (4)$$

where $\mathcal{U}(\mathbf{Q}) := \{Q_{ij} : i, j \in [n]\}$. Note that always $0 \in \mathcal{U}(\mathbf{Q})$, since \mathbf{Q} is upper triangular, that is $Q_{ij} = 0$ for $i > j$. A large DR indicates that many bits are required to represent all parameters of \mathbf{Q} accurately in binary, as the parameters span a wide range of values and require fine gradations. Taking the next larger integer larger than the DR quantifies how many *bits* are required to faithfully implement the parameters of a QUBO.

Another measure for describing the required precision is the *maximum coefficient ratio* (Stollenwerk et al. 2019)

$$C_{\max}(\mathbf{Q}) := \frac{\max \mathcal{U}(\mathbf{Q})}{\min \mathcal{U}(\mathbf{Q}) \setminus \{0\}} \leq 2^{\text{DR}(\mathbf{Q})}. \quad (5)$$

That is to say, we understand DR as a measure of representational complexity. Even though C_{\max} might be very small, the DR can still be large, but the reverse does not hold.

3 Methodology

Our main goal is to reduce the DR of a given QUBO problem by transforming the corresponding QUBO matrix subject to the requirement that a global optimizers must be kept intact. To this end, we define the notion of *optimum inclusion* (\sqsubseteq) on QUBO instances as $\mathbf{Q} \sqsubseteq \mathbf{Q}' \Leftrightarrow \mathcal{Z}^*(\mathbf{Q}) \subseteq \mathcal{Z}^*(\mathbf{Q}')$. We formulate the problem as follows:

$$\arg \min_{\mathbf{A} \in \mathcal{Q}_n} \text{DR}(\mathbf{Q} + \mathbf{A}) \quad (6a)$$

$$\text{s.t. } \mathbf{Q} + \mathbf{A} \sqsubseteq \mathbf{Q}. \quad (6b)$$

Let us give a small example for clarification.

Example 1. Consider the following 2×2 matrices:

$$\mathbf{Q} = \begin{bmatrix} 0.8 & -1.5 \\ 0 & -1000 \end{bmatrix}, \quad \mathbf{Q}' = \begin{bmatrix} 0.8 & -1.5 \\ 0 & -2 \end{bmatrix}.$$

Observing the corresponding QUBO problems, we get

$$\arg \min_{\mathbf{z} \in \{0, 1\}^2} \mathbf{z}^{\top} \mathbf{Q} \mathbf{z} = \arg \min_{\mathbf{z} \in \{0, 1\}^2} \mathbf{z}^{\top} \mathbf{Q}' \mathbf{z} = \begin{pmatrix} 1 \\ 1 \end{pmatrix},$$

that is, \mathbf{Q} and \mathbf{Q}' have the same optimizer, therefore $\mathbf{Q} \sqsubseteq \mathbf{Q}'$. Furthermore, it holds that

$$\mathbf{Q} + \mathbf{A} = \mathbf{Q}', \quad \mathbf{A} := \begin{bmatrix} 0 & -998 \\ 0 & 0 \end{bmatrix}$$

When we compare the DR of \mathbf{Q} and \mathbf{Q}' , we find that $\text{DR}(\mathbf{Q}) \approx 10.29$, $\text{DR}(\mathbf{Q}') \approx 2.49$.

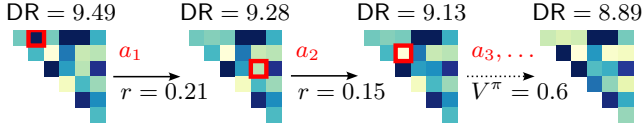


Figure 1: Illustration of the MDP described in Section 3. Every step t , we choose an action a_t in form of an index pair and update our state s_t to s_{t+1} to obtain a matrix with a smaller DR. The goal is to maximize the value function V^π .

3.1 MDP Formulation

We consider the state space as $\mathbb{S} = \mathcal{Q}_n$ and the action space $\mathbb{A} := [n] \times [n]$. The state transition function is given by

$$f(s, a) = f(\mathbf{Q}, (k, l)) = \mathbf{Q} + h(\mathbf{Q}, (k, l))\mathbf{e}_k\mathbf{e}_l^\top, \quad (7)$$

and we define the reward function as

$$r(s, a) = \text{DR}(s) - \text{DR}(f(s, a)). \quad (8)$$

Here, $h : \mathcal{Q}_n \times [n] \times [n] \rightarrow \mathbb{R}$, is a function for determining the parameter update. The 4-tuple $(\mathbb{S}, \mathbb{A}, f, r)$ defines a Markov Decision Process (MDP).

For f , we consider the following heuristic h (Mücke, Gerlach, and Piatkowski 2023) (which we also denote by G): Matrix entries Q_{kl} are changed in a greedy fashion by some parameter w_{kl} , $Q_{kl} \rightarrow Q_{kl} + w_{kl}$ with $k, l \in [n]$, $k \leq l$ such that one global optimizer is preserved, i.e.,

$$y_{kl}^-(\mathbf{Q}) \leq w_{kl} \leq y_{kl}^+(\mathbf{Q}) \Rightarrow \mathbf{Q} + w_{kl}\mathbf{e}_k\mathbf{e}_l^\top \sqsubseteq \mathbf{Q}, \quad (9)$$

where $\mathbf{e}_k, \mathbf{e}_l$ are the standard basis vectors with zeros everywhere except at index k and l , respectively. Note that $y_{kl}^-(\mathbf{Q}) \leq 0 \leq y_{kl}^+(\mathbf{Q})$. The procedure is illustrated in Fig. 3a. Now assume that we want to change T QUBO matrix entries such that the accumulated reward is maximized. Formally, the goal is to find a policy $\pi^* : \mathbb{S} \rightarrow \mathbb{A}$, s.t.,

$$\pi^* = \arg \max_{\pi : \mathbb{S} \rightarrow \mathbb{A}} V^\pi(s_0) = \arg \max_{\pi : \mathbb{S} \rightarrow \mathbb{A}} \sum_{t=0}^{T-1} r(s_t, \pi(s_t)) \quad (10a)$$

$$= \arg \min_{\pi : \mathbb{S} \rightarrow \mathbb{A}} \text{DR}(f_T(\mathbf{Q}, \pi)), \quad (10b)$$

where the equality follows through a telescopic sum and the t -time state transition f_t following policy π is defined as

$$f_t(s_0, \pi) := f(s_t, \pi(s_t)) = s_{t+1}, \quad s_0 := \mathbf{Q}. \quad (11)$$

Our MDP is illustrated in Fig. 1. Observing that the transition Eq. (7) is a simple matrix addition, we can write $f_T(\mathbf{Q}, \pi) = \mathbf{Q} + \mathbf{A}'$, where $\mathbf{Q} + \mathbf{A}' \sqsubseteq \mathbf{Q}$. Thus, the optimization objective of the decision process in Eq. (10) is a more restricted version of the problem in Eq. (6). That is, we do not optimize over the set of all optimum inclusive matrices, but over the subset of matrices which can be created with any policy following our MDP framework. The cumulative sum in Eq. (10a) is also called the value function V^π for a policy π . Using the recursive Bellman equation

$$V^{\pi^*}(s_t) = \max_{a \in \mathbb{A}} [r(s_t, a) + V^{\pi^*}(f(s_t, a))], \quad (12)$$

we can find an optimal policy in Eq. (10) with dynamic programming (DP), using a shortest path-type method. In our

Algorithm 1 BRANCHANDBOUND

Input: $\mathbf{Q}, T, \tilde{T}, r^*$

Output: New candidates \mathcal{Q} and new best upper bound \hat{r}

```

1:  $\mathcal{Q} \leftarrow \{\}$ 
2:  $\mathcal{I} \leftarrow \text{GETINDICES}(\mathbf{Q})$ 
3: for  $(k, l)$  in  $\mathcal{I}$  do ▷ Branch step
4:    $\mathbf{Q}' \leftarrow \text{NEXTSTATE}(\mathbf{Q}, T, \tilde{T}, (k, l))$ 
5:    $r^* \leftarrow \min\{r^*, \text{DR}(f_T(\mathbf{Q}, \pi))\}$  ▷ Update  $r^*$ 
6:   if  $r^* \geq \text{LOWERBOUND}(\mathbf{Q}', T)$  then ▷ Bound step
7:      $\mathcal{Q} \leftarrow \mathcal{Q} \cup \{\mathbf{Q}'\}$ 
8:   end if
9: end for
```

Algorithm 2 NEXTSTATE

Input: $\mathbf{Q}, T, \tilde{T}, (k, l)$

Output: New candidate \mathbf{Q}'

```

1:  $\mathbf{Q}' \leftarrow f(\mathbf{Q}, (k, l))$  ▷ Next state
2: if  $T - 1 = \tilde{T}$  then ▷ Policy rollout
3:   for  $t = 1$  to  $\tilde{T}$  do
4:      $(i, j) \leftarrow \pi(\mathbf{Q}')$ 
5:      $\mathbf{Q}' \leftarrow f(\mathbf{Q}, (i, j))$ 
6:   end for
7: end if
```

case, we have no knowledge about the final state $f_T(\mathbf{Q}, \pi)$ and thus the search space is exponentially large (see Fig. 2). Choosing the number of iterations T logarithmic in the problem dimension, i.e., $T = \log_2(n^2) = 2 \log_2(n)$, results in a sub-exponential ($o(2^n)$) state space size. Thus, we have an asymptotically slower growth than the exponentially large state space size 2^n of the original QUBO problem. However, in practice, super-polynomial runtimes are often not tractable, especially for large n . Due to this fact, Eq. (12) is typically solved with approximate DP methods such as Monte Carlo Tree Search (MCTS), policy rollout (PR) or reinforcement learning (Bertsekas 2019, 2021).

Next, we present a *Branch and Bound* (B&B) algorithm utilizing PR to reduce the complexity of solving Eq. (10).

4 Branch and Bound

Following all paths of possible QUBO matrix updates is intractable. We combine PR with the B&B paradigm to obtain a trade-off between computational complexity and solution quality—solution paths which cannot lead to an optimum are pruned, based on bounds on the best found solution.

The algorithm is given in Fig. 2: the search space is expanded (branch, Line 3) and every state is checked whether it can be pruned (bound, Line 6) in Algorithm 1. This is done recursively until the final horizon T is reached and the state with the minimum DR is returned.

4.1 Branch

In the *branch*-step, the search space is expanded from the current considered state. The method GETINDICES (Line 2, Algorithm 1) decides which indices to consider in the current iteration, i.e., which entries of QUBO matrix should be changed. The most obvious version is of course to use all

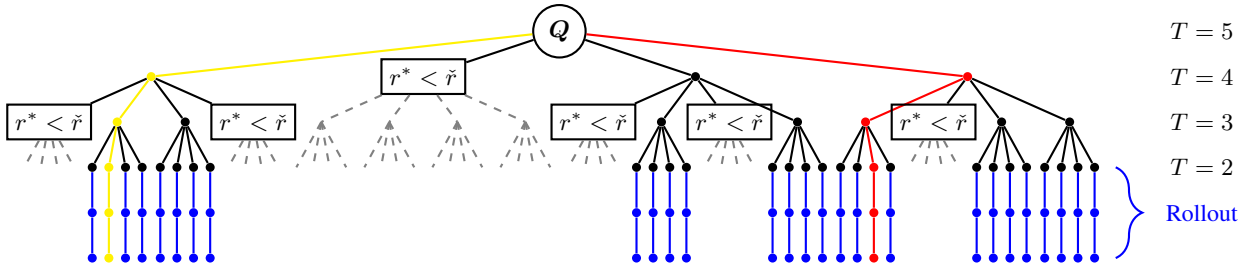


Figure 2: Exemplary depiction of the search space when applying our B&B algorithm (Section 4) to some QUBO matrix Q . In every step, we expand our search space (from top to bottom, Section 4.1) and check whether a branch can be pruned ($r^* < \tilde{r}$, Section 4.3). The small filled circles indicate the visited states of our algorithm and the pruned parts are depicted as gray dashed lines. The fraction of pruned states is $40/85 = 0.47$ (without rollout). Since the search space size grows exponentially with the horizon $T = 5$, we execute a PR (Section 4.2) for $\tilde{T} = 2$ steps. From here on, a base policy is followed without expanding further, which is depicted in blue. The red path indicates the optimal solution and the yellow path shows the base policy.

indices $[n] \times [n]$ of the whole matrix, which we will further indicate by ALL. With large n , this expansion gets very large and thus we also consider a different method in our experiments. This method is based on the observation, that only four entries of the QUBO matrix affect the DR when changing a single weight. Namely the smallest/largest weight and the weights which are closest to each other, which will be denoted by IMPACT. This drastically reduces size of the search space for large n and the performance to considering all weights is compared in Section 5.

4.2 Policy Rollout

Having an index pair (k, l) at hand, a new state is created from the current state Q by following the transition function in Eq. (7) (Algorithm 2, Line 1). Instead of solving the problem in Eq. (10) exactly and expanding the search space for T steps, we also consider a PR approach. It describes the concept of following a given a base policy $\hat{\pi}$ for a number of steps. For a given rollout depth $\tilde{T} \leq T$, we denote the policy which optimizes its path for \tilde{T} steps and then follows $\hat{\pi}$ for $T - \tilde{T}$ steps as $\tilde{\pi}_{\tilde{T}}$. We use a greedy policy

$$\hat{\pi}(Q) := \arg \min_{a \in \mathbb{A}} \text{DR}(f(Q, a)), \quad (13)$$

which myopically optimizes the DR when taking a single step. Since the solution quality is monotonically increasing with \tilde{T} , we obtain a trade-off between the size of the state space and the performance of our algorithm.

Using PR is motivated by the well known *rollout selection policy*. At time t , the optimal future reward $V^{\pi^*}(f(s_t, a))$ is approximated with the reward $V^{\hat{\pi}}(f(s_t, a))$ following $\hat{\pi}$. The Bellman equation Eq. (12) is modified to

$$V^{\tilde{\pi}}(s_t) = \max_{a \in \mathbb{A}} \left[r(s_t, a) + V^{\hat{\pi}}(f(s_t, a)) \right]. \quad (14)$$

The resulting rollout selection policy $\tilde{\pi}$ is at least equal and typically better than the base policy $\hat{\pi}$. It is renowned for its simplicity and strong performance, largely due to its close relationship with the fundamental dynamic programming algorithm of policy iteration. Eq. (14) represents the optimal one-step look-ahead policy, when subsequently following

a base policy. This principle can be generalized to \tilde{T} -step look-ahead rollouts, $\tilde{T} \leq T$, where the solution quality increases with increasing rollout horizon \tilde{T} . The exact solution for Eq. (10) is obtained if $\tilde{T} = T$. Thus, PR can be seamlessly integrated into our B&B algorithm.

There are several variants of the rollout selection policy for reducing computational requirements. *Simplified rollout* is employed to reduce the action space size in every step by choosing a subset due to some measure. Note that simplified rollout bears some resemblance to the *beam search* method (Steinbiss, Tran, and Ney 1994) for exploration, where a fixed-size search beam is maintained for traversing through the search space. Another way of reducing computational burden is to use *truncated rollout*. In the latter case, the policy rollout is stopped earlier than using the full horizon.

An experimental comparison between $\tilde{\pi}_{\tilde{T}}$ and $\hat{\pi}$ with using the aforementioned variants can be found in Section 5.1.

4.3 Bound

We want to prune states, which cannot lead to the optimal solution. Deciding whether a state can be pruned, is dependent on bounds of the reachable best solution from that given state. Given the current best final DR r^* , we can prune a state Q if it is smaller than a lower bound $\tilde{r}(Q, T)$ on the best reachable solution $\text{DR}(f_T(Q, \pi^*))$ (Line 6, Algorithm 1)

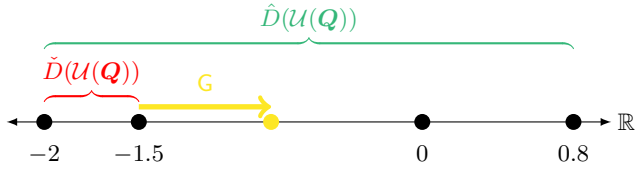
$$r^* \leq \tilde{r}(Q, T) \leq \text{DR}(f_T(Q, \pi^*)). \quad (15)$$

Pruning states, we do not have to expand the search further and can drastically reduce the computation time.

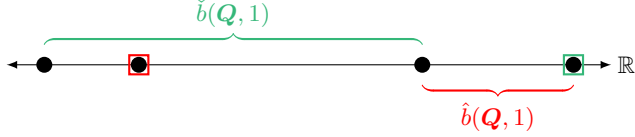
An upper bound $\hat{r}(Q, T) \geq \text{DR}(f_T(Q, \pi^*))$ can be found by iteratively following a base policy $\hat{\pi}$ for T steps (PR) to reduce the DR. r^* is set to this upper bound when $r^* < \hat{r}(Q, T)$ (Line 5, Algorithm 1). We find a lower bound on $\text{DR}(f_T(Q, \pi^*))$ by finding a lower bound on the nominator $\hat{D}(\mathcal{U}(f_T(Q, \pi^*))) \geq \hat{b}(Q, T)$ and an upper bound on the denominator $\hat{D}(\mathcal{U}(f_T(Q, \pi^*))) \leq \hat{b}(Q, T)$ in Eq. (4). Then

$$\text{DR}(f_T(Q, \pi^*)) \geq \log_2 \left(\frac{\hat{b}(Q, T)}{\hat{b}(Q, T)} \right) =: \tilde{r}(Q, T). \quad (16)$$

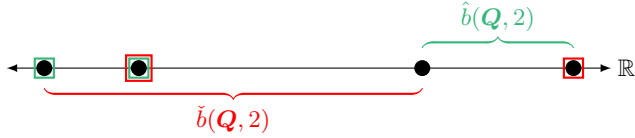
Let $m := n^2$ be the number of entries of an $n \times n$ matrix.



(a) We can read off $\hat{D}(U(Q)) = 2.8$ (red) and $\tilde{D}(U(Q)) = 0.5$ (green). Change of parameter Q_{01} using a heuristic $G(Q, 0, 1) = 0.7$ (yellow). The sorted parameters are given by $q_1 = -2$, $q_2 = -1.5$, $q_3 = 0$ and $q_4 = 0.8$.



(b) Bounds when a single QUBO parameter is changed to 0: A lower bound (top, green) is given by $\tilde{D}(U(f_1(Q, \pi^*))) \geq \tilde{b}(Q, 1) = 2$ and an upper bound (bottom, red) by $\tilde{D}(U(f_1(Q, \pi^*))) \leq \hat{b}(Q, 1) = 0.8$. The changed parameters are indicated with rectangular boxes.



(c) Bounds when two QUBO parameters are changed, namely $\tilde{b}(Q, 2) = 0.8$ and $\hat{b}(Q, 2) = 2$. For details, see Fig. 3b.

Figure 3: Sorted QUBO parameters of the matrix given in Example 1. The heuristics are depicted in Fig. 3a and the two methods for finding a lower bound on the DR are given in Figs. 3b and 3c.

For any $Q \in \mathcal{Q}_n$, there is an ordering (bijective map) $\sigma : [m] \rightarrow [n] \times [n]$ of entries such that

$$q_\ell \leq q_{\ell+1}, q_\ell \equiv Q_{\sigma(\ell)}, \forall \ell \in [m]. \quad (17)$$

With this notation, $\hat{D}(U(Q)) = q_m - q_1$ and $\exists j \in [m-1] : \tilde{D}(U(Q)) = q_{j+1} - q_j$. A visualization for an ordering of Example 1 is shown in Fig. 3a.

Lower Bound on Maximum Distance For finding a lower bound on $\text{DR}(f_T(Q, \pi^*))$, we optimistically assume that we can set all parameters to 0 while maintaining an optimizer of Q . Since 0 is always considered in the computation of the DR, this corresponds to an optimal strategy of changing the parameters, because the DR cannot increase. Changing a single parameter, $\hat{D}(U(Q))$ is maximally reduced if we either set q_1/q_m larger/smaller than q_2/q_{m-1} . The maximum possible reduction is equal to $\min\{q_2 - q_1, q_m - q_{m-1}\}$. Iterating this process for T times, we end up with

$$\tilde{b}(Q, T) := \min \{q_{m-T+i} - q_{i+1} \mid 0 \leq i \leq T\}. \quad (18)$$

An illustration for Example 1 is found in Figs. 3b and 3c.

Upper Bound on Minimum Distance Obtaining a lower bound is a little more tricky and an iterative procedure is

Algorithm 3 LOWERBOUND

Input: Q, T

Output: Lower bound $\tilde{r} \leq \text{DR}(U(Q_T^{\pi^*}))$

```

1:  $\tilde{b} \leftarrow \min \{q_{m-T+i} - q_{i+1} \mid 0 \leq i \leq T\}$ 
2: Compute  $\sigma$ , s.t.,  $q_\ell \leq q_{\ell+1}$ ,  $q_\ell \equiv Q_{\sigma(\ell)}$  ▷ Eq. (17)
3:  $\bar{\mathcal{D}} \leftarrow \{d_i \mid i \in [m-1]\}_b$ ,  $d_i = q_{i+1} - q_i$ 
4: Compute  $\rho$ , s.t.,  $d_{\rho(\ell)} \leq d_{\rho(\ell+1)}$ 
5: for  $t = 1$  to  $T$  do
6:    $\mathcal{I} \leftarrow \{\rho(1), \rho(1) + 1\}$ 
7:    $i_* = \arg \min_{i \in \mathcal{I}} d_i$ 
8:   if  $i_* = \rho(1)$  then
9:      $i_* \leftarrow i_* - 1$ 
10:  end if
11:   $d_{i_*} \leftarrow d_{i_*} + d_{\rho(1)}$  ▷ Update distance
12:   $\bar{\mathcal{D}} \leftarrow \bar{\mathcal{D}} \setminus \{d_{\rho(1)}\}$ 
13:  Recompute  $\rho$ , s.t.,  $d_{\rho(\ell)} \leq d_{\rho(\ell+1)}$ 
14: end for
15:  $\tilde{b} \leftarrow d_{\rho(1)}$ 
16:  $\tilde{r} \leftarrow \tilde{b}/\hat{b}$ 

```

given in Algorithm 3. Since we are concerned with the smallest distance between two QUBO parameters, we consider the set of distances between “neighboring” parameters $\bar{\mathcal{D}}(U(Q)) := \{q_{i+1} - q_i \mid i \in [m-1]\} = \{d_i \mid i \in [m-1]\}$. Define an ordering $\rho : [m-1] \rightarrow [m-1]$, s.t., $d_{\rho(i)} \leq d_{\rho(i+1)}$. It then holds that $\tilde{D}(U(Q)) = d_{\rho(1)}$. $\tilde{D}(U(Q))$ is maximally reduced if we change $q_{\rho(1)+1}$ or $q_{\rho(1)}$, s.t., $d_{\rho(1)}$ is not the smallest distance anymore. We change the weight with the smaller corresponding distance (Lines 6 and 7, Algorithm 3). However, if one of the weights equals 0, we choose the other one, since 0 will always be considered in the distance computation. If $q_{\rho(1)}$ is changed, $d_{\rho(1)-1}$ is updated to $d_{\rho(1)-1} + d_{\rho(1)} = q_{\rho(1)+1} - q_{\rho(1)-1}$ and if $q_{\rho(1)+1}$ is changed, $d_{\rho(1)+1}$ is updated to $d_{\rho(1)+1} + d_{\rho(1)} = q_{\rho(1)+2} - q_{\rho(1)}$ (Line 11, Algorithm 3). No update is required if $\rho(1) = 1$ or $\rho(1) + 1 = m$. The new smallest distance either equals the second smallest distance $d_{\rho(2)}$ or one of the two newly updated ones. The smallest distance $d_{\rho(1)}$ is removed (Line 12, Algorithm 3) from $\bar{\mathcal{D}}$ and the ordering ρ is updated with the updated distances (Line 11, Algorithm 3). In Figs. 3b and 3c, this is illustrated for Example 1.

The computational complexity of our bounds is derived and discussed in the Appendix.

5 Experiments

In what follows, we consider a numerical experiments and study the impact of our method on a D-Wave Advantage System 5.4 quantum annealer (QA). Three exemplary problems are considered: BINCLUSTERING represents 2-means clustering, SUBSETSUM consists of finding a subset from a list of values that sum up to a given target value and MRF consists of maximum a posteriori state inference in an undirected graphical model. All three problems have known QUBO embeddings (Bauckhage et al. 2018; Biesner et al. 2022; Mücke, Piatkowski, and Morik 2019). The specific setups are described in the Appendix.

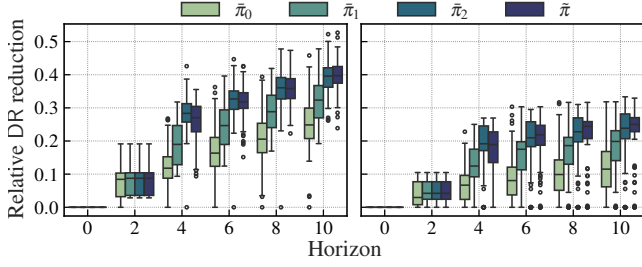


Figure 4: Relative DR reduction for 100 $n = 8$ (left) and $n = 16$ (right) BINCLUSTERING instances. Different policies are compared for choosing the indices in Algorithm 1 with ALL.

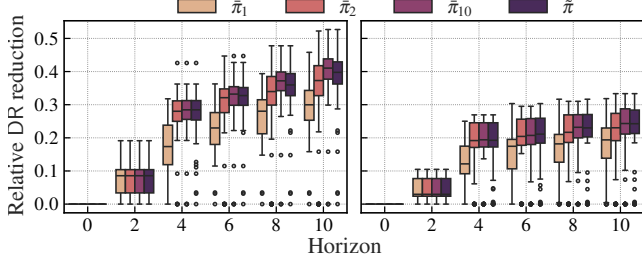


Figure 5: Relative DR reduction for 100 $n = 8$ (left) and $n = 16$ (right) BINCLUSTERING instances. Different policies are compared for choosing the indices in Algorithm 1 with IMPACT.

5.1 Numerical Experiments

We compare different policies: the base policy $\hat{\pi}$, the B&B policy $\hat{\pi}_{\tilde{T}}$ with different rollout horizons \tilde{T} and the rollout selection policy $\tilde{\pi}$. The relative DR reduction for a horizon up to $T = 10$ can be found in Fig. 4. We compare the two methods ALL (Fig. 4) and IMPACT (Fig. 5) for choosing the indices in the branch step (Line 3, Algorithm 1). It is apparent that every single policy reduces the DR with an increasing horizon T . The base policy $\hat{\pi}$ is largely outperformed by $\hat{\pi}_{\tilde{T}}$ and $\tilde{\pi}$. $\hat{\pi}_{\tilde{T}}$ is increasing its performance with an increasing rollout horizon \tilde{T} . We can see that the exact method ALL has the same performance as using the simplified version IMPACT, while being more computational demanding. While ALL scales quadratically with the problem size n , IMPACT is basically independent of n . Furthermore, the rollout selection policy $\tilde{\pi}$ already almost achieves optimal performance (c.f. to $\hat{\pi}_{10}$). We also evaluate our results with the maximum coefficient ratio C_{\max} Eq. (5) for $n = 8$. It is evident from Fig. 6, that $C_{\max}(Q) \leq \text{DR}(Q)$, aligning with our theoretical insights. We can see that with our algorithm C_{\max} is also reduced. Evaluating the quality of our bounds (see Section 4.3), we indicate the fraction of the pruned state space in Fig. 7. We here consider the exact solution, that is $\hat{\pi}_T$. We vary the depth until the upper bounds are updated (Line 5, Algorithm 1). Increasing this depth, as well as increasing the horizon leads to pruning a larger fraction of the whole search space. Furthermore, the number of pruned states does not heavily depend on an updated current best,

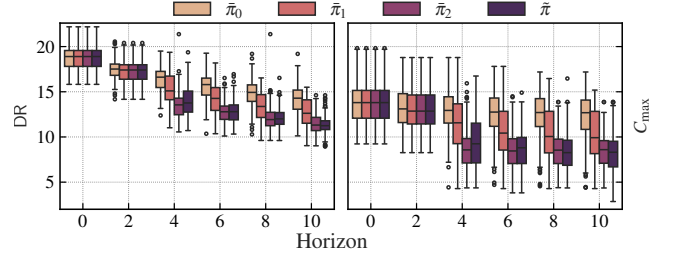


Figure 6: Comparison between absolute DR and C_{\max} reduction for $n = 8$ and IMPACT indices.

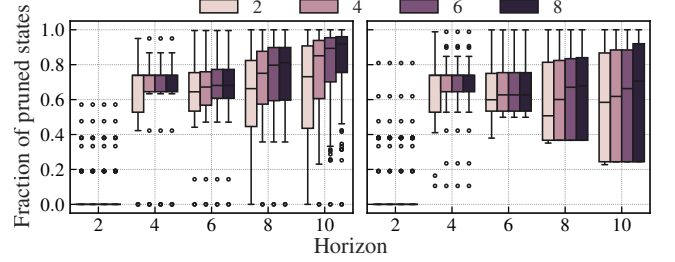


Figure 7: Fraction of pruned states compared. Different depths (2, 4, 6 and 8) for updating the current best DR (Line 5, Algorithm 1) are compared for $n = 8, 16$.

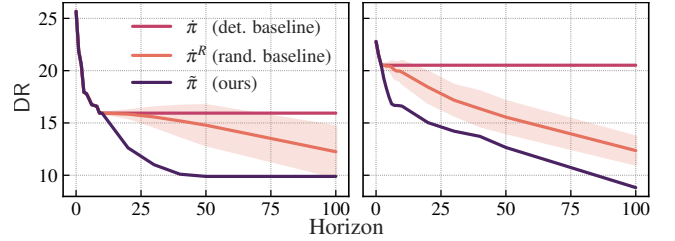


Figure 8: Performance of our developed policy $\tilde{\pi}$ compared to the base policy $\hat{\pi}$ and the randomized base policy $\hat{\pi}^R$. The DR reduction is compared for a SUBSETSUM (left) and a BINCLUSTERING (right) instance.

indicating the strength of our lower bound (Section 4.3).

5.2 Performance on Hardware Solvers

We assess the impact of the reduced QUBO instances on a real QA. Due to its probabilistic nature, we generate 1000 *samples* and use default parameters. First, we consider the SUBSETSUM and BINCLUSTERING problems. For both, we compare the reduction performance of the base policy $\hat{\pi}$ and a randomized base policy $\hat{\pi}^R$ with our rollout selection policy $\tilde{\pi}$. Standard deviations are shown in Fig. 8. For the SUBSETSUM instance the initial DR of the QUBO matrix is 25.676 and $\hat{\pi}$ gets stuck in a local optimum after already $T = 9$ steps with a DR of 15.939. However, our $\tilde{\pi}$ is steadily improving with an increasing horizon. For making the performances comparable we evaluate the original QUBO energy $E_Q(z)$ for every sample z and have a look at the relative distance to the optimum energy ($(E_Q(z) -$

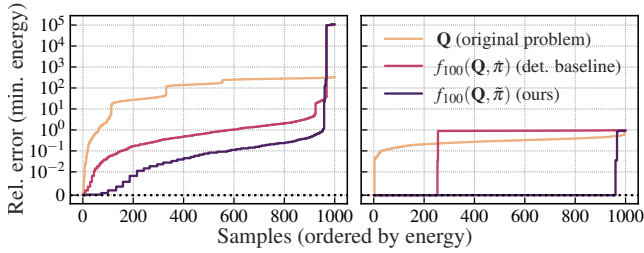


Figure 9: Performance the D-Wave Advantage 5.4 for different QUBO instances: the original QUBO Q , the QUBO using the base policy for 100 steps $f_{100}(Q, \tilde{\pi})$ and the QUBO using the rollout selection policy for 100 steps $f_{100}(Q, \tilde{\pi})$. The relative QUBO energies for 1000 samples are shown for a SUBSETSUM (left) and a BINCLUSTERING (right) instance.

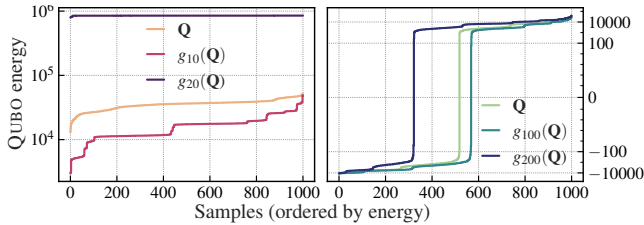


Figure 10: Performance the D-Wave Advantage 5.4 for different Iris and MNIST QUBO instances: the original QUBO Q , the QUBO using the heuristic g for 10 and 20 steps for Iris and 100 and 200 steps for MNIST, respectively. The relative QUBO energies for 1000 samples are shown for Iris (left) and MNIST predicting digit 0 (right).

$E_Q(z^*)/E_Q(z)$). This is depicted in Fig. 9, where we indicate the energy distribution for the initial QUBO matrix Q , the base policy $f_{100}(Q, \tilde{\pi})$ and the rollout selection policy $f_{100}(Q, \tilde{\pi})$. Furthermore, we depict the median of the relative energies along with the number of optimal samples in Table 1. Remember that our proposed DR reduction method preserves the solution vectors while altering the parameter values, which can significantly change the energy landscape of the reduced QUBO compared to the original. This is evident from the *worst* samples (highest energy) of the reduced QUBO problems, which are way larger than the original ones. Moreover, for the BINCLUSTERING instance, the median of the energy distribution of $f_{100}(Q, \tilde{\pi})$ is larger than the one from Q ($0.91 > 0.30$), even though the DR is smaller ($20.519 < 22.792$). However, the low energy values are more interesting since we aim to minimize the energy.

Next, we want to investigate how important it is, to preserve an optimum while reducing the DR. Instead of using our optimum preserving MDP framework, we investigate the effect on the solution quality of the quantum annealer using a different heuristic. That is, we incrementally reduce the DR by using the algorithms given in Section 4.3. We refer to the Appendix for more details. We denote this heuristic operating for T steps on Q as $g_T(Q)$. Scaling things up a little, We consider QUBO implementations of probabilistic inference on the Iris dataset (Fisher 1988) and on MNIST (Deng

	SUBSETSUM			BINCLUSTERING		
	Energy	#Opt	DR	Energy	#Opt	DR
Orig	157.39	0	25.68	0.30	3	22.79
Base	0.72	0	15.94	0.91	253	20.52
Ours	0.08	16	9.88	0	960	8.18

Table 1: Comparison of median rel. energy, number of optimal samples (#Opt), and DR for the original QUBO Q (Orig), the base line $f_{100}(Q, \tilde{\pi})$ (Base), and our rollout selection policy $f_{100}(Q, \tilde{\pi})$ (Ours).

	Iris			MNIST		
Q	$g_{10}(Q)$	$g_{20}(Q)$		Q	$g_{100}(Q)$	$g_{200}(Q)$
21.80	15.03	12.41		59.58	22.42	21.31

Table 2: DR comparison of the original QUBO Q and the ones obtained using different horizons for g for MRF QUBO embeddings for Iris and MNIST.

2012). This leads to QUBO instances of dimension $n = 216$ for Iris and $n = 696$ for MNIST. For Iris, our method reduced the DR from 21.80 to 12.41 and for MNIST from 59.58 to 21.31. In Fig. 10, the performance of the quantum annealer for these QUBO problems is depicted, where we show the energy distribution similar to Fig. 9. The corresponding DR can be found in Table 2. We can see that a reduced DR leads to a better performance on real quantum hardware. However, when we change the QUBO landscape too much with g (large horizon), a global optimum is not preserved anymore and the performance largely deteriorates.

6 Conclusion

In this paper, we developed a principled Branch-and-Bound algorithm for reducing the required precision for quadratic unconstrained binary optimization problems (QUBO). In order to do this, we consider the dynamic range (DR) as a measure of required precision, which we iteratively reduce in a Markov Decision Process (MDP) framework. We propose computationally efficient (quadratically in problem size) and theoretically sound bounds for pruning, leading to drastic reduction of the search space size. Furthermore, we combine our approach with the well-known policy rollout for improving computational efficiency and the performance of already existing heuristics. Our extensive experiments comply with the theoretical insights. We use our method to reduce the DR of NP-hard real-world problems, such as clustering and subset sum. Our proposed algorithm largely outperforms recently developed greedy heuristics. The reduced QUBO instances are then solved with a real quantum annealer (QA). We conclude that our method enhances the reliability of a QA in finding the optimum, as the *Integrated Control Errors* constrain the dynamic range of the hardware parameters.

In future work, it would be very interesting to investigate further techniques for approximate dynamic programming, such as reinforcement learning. Since our MDP is determin-

stic and the action space is discrete, Q -learning can be of great benefit to learn different base policies, other than the greedy approach. This could then easily be fit into our framework. Furthermore, evaluation of the effect of our algorithm for using different hardware, such as GPUs, FPGAs or coherent Ising machines is very intriguing.

References

- Albasha, T.; and Lidar, D. A. 2018. Adiabatic quantum computation. *Reviews of Modern Physics*, 90(1): 015002.
- Aloise, D.; Deshpande, A.; Hansen, P.; and Papat, P. 2009. NP-hardness of Euclidean sum-of-squares clustering. *Machine Learning*, 75(2): 245–248.
- Bauckhage, C.; Ojeda, C.; Sifa, R.; and Wrobel, S. 2018. Adiabatic Quantum Computing for Kernel $k=2$ Means Clustering. In *LWDA*, 21–32.
- Bertsekas, D. 2019. *Reinforcement learning and optimal control*, volume 1. Athena Scientific.
- Bertsekas, D. 2021. *Rollout, policy iteration, and distributed reinforcement learning*. Athena Scientific.
- Bertsekas, D. P.; Tsitsiklis, J. N.; and Wu, C. 1997. Roll-out algorithms for combinatorial optimization. *Journal of Heuristics*, 3: 245–262.
- Biesner, D.; Gerlach, T.; Bauckhage, C.; Kliem, B.; and Sifa, R. 2022. Solving subset sum problems using quantum inspired optimization algorithms with applications in auditing and financial data analysis. In *2022 21st IEEE International Conference on Machine Learning and Applications (ICMLA)*, 903–908. IEEE.
- Brown, G. 2009. A New Perspective for Information Theoretic Feature Selection. In van Dyk, D.; and Welling, M., eds., *Proceedings of the Twelfth International Conference on Artificial Intelligence and Statistics*, volume 5 of *Proceedings of Machine Learning Research*, 49–56. Hilton Clearwater Beach Resort, Clearwater Beach, Florida USA: PMLR.
- Chai, Y.; Funcke, L.; Hartung, T.; Jansen, K.; Kühn, S.; Stornati, P.; and Stollenwerk, T. 2023. Optimal Flight-Gate Assignment on a Digital Quantum Computer. *Physical Review Applied*, 20(6).
- Choukroun, Y.; Kravchik, E.; Yang, F.; and Kisilev, P. 2019. Low-bit Quantization of Neural Networks for Efficient Inference. In *International Conference on Computer Vision Workshops*, 3009–3018. IEEE.
- Deng, L. 2012. The mnist database of handwritten digit images for machine learning research. *IEEE Signal Processing Magazine*, 29(6): 141–142.
- Ermon, S.; Gomes, C. P.; Sabharwal, A.; and Selman, B. 2013. Taming the Curse of Dimensionality: Discrete Integration by Hashing and Optimization. In *International Conference on Machine Learning*, volume 28 of *JMLR Workshop and Conference Proceedings*, 334–342. JMLR.org.
- Fisher, R. A. 1988. Iris. UCI Machine Learning Repository. DOI: <https://doi.org/10.24432/C56C76>.
- Glover, F.; and Laguna, M. 1998. *Tabu search*. Springer.
- Goldberg, D. E.; and Kuo, C. H. 1987. Genetic algorithms in pipeline optimization. *Journal of Computing in Civil Engineering*, 1(2): 128–141.
- Kagawa, H.; Ito, Y.; Nakano, K.; Yasudo, R.; Kawamata, Y.; Katsuki, R.; Tabata, Y.; Yazane, T.; and Hamano, K. 2020. Fully-pipelined architecture for simulated annealing-based QUBO solver on the FPGA. In *2020 Eighth International Symposium on Computing and Networking (CANDAR)*, 39–48. IEEE.
- Kirkpatrick, S.; Gelatt Jr, C. D.; and Vecchi, M. P. 1983. Optimization by simulated annealing. *science*, 220(4598): 671–680.
- Kochenberger, G.; Hao, J.-K.; Glover, F.; Lewis, M.; Lü, Z.; Wang, H.; and Wang, Y. 2014. The unconstrained binary quadratic programming problem: a survey. *Journal of combinatorial optimization*, 28: 58–81.
- Lucas, A. 2014. Ising formulations of many NP problems. *Frontiers in physics*, 2: 74887.
- Mastiyage Don, S. H. G.; Inui, Y.; Kako, S.; Yamamoto, Y.; and Aonishi, T. 2023. Mean-field coherent Ising machines with artificial Zeeman terms. *Journal of Applied Physics*, 134(23).
- Matsubara, S.; Takatsu, M.; Miyazawa, T.; Shibasaki, T.; Watanabe, Y.; Takemoto, K.; and Tamura, H. 2020. Digital annealer for high-speed solving of combinatorial optimization problems and its applications. In *2020 25th Asia and South Pacific Design Automation Conference (ASP-DAC)*, 667–672. IEEE.
- Mohseni, N.; McMahon, P. L.; and Byrnes, T. 2022. Ising machines as hardware solvers of combinatorial optimization problems. *Nature Reviews Physics*, 4(6): 363–379.
- Mücke, S.; Gerlach, T.; and Piatkowski, N. 2023. Optimum-Preserving QUBO Parameter Compression. *arXiv preprint arXiv:2307.02195*.
- Mücke, S.; Heese, R.; Müller, S.; Wolter, M.; and Piatkowski, N. 2023. Feature selection on quantum computers. *Quantum Machine Intelligence*, 5(1): 11.
- Mücke, S.; Piatkowski, N.; and Morik, K. 2019. Learning Bit by Bit: Extracting the Essence of Machine Learning. In *LWDA*, 144–155.
- Narendra; and Fukunaga. 1977. A branch and bound algorithm for feature subset selection. *IEEE Transactions on computers*, 100(9): 917–922.
- Pardalos, P. M.; and Jha, S. 1992. Complexity of Uniqueness and Local Search in Quadratic 0–1 Programming. *Operations research letters*, 11(2): 119–123.
- Punnen, A. P. 2022. The quadratic unconstrained binary optimization problem. *Springer International Publishing*, 10: 978–3.
- Rehfeldt, D.; Koch, T.; and Shinano, Y. 2023. Faster exact solution of sparse MaxCut and QUBO problems. *Mathematical Programming Computation*, 15(3): 445–470.
- Silver, D.; Huang, A.; Maddison, C. J.; Guez, A.; Sifre, L.; Van Den Driessche, G.; Schrittwieser, J.; Antonoglou, I.; Panneershelvam, V.; Lanctot, M.; et al. 2016. Mastering the

game of Go with deep neural networks and tree search. *nature*, 529(7587): 484–489.

Steinbiss, V.; Tran, B.-H.; and Ney, H. 1994. Improvements in beam search. In *ICSLP*, volume 94, 2143–2146.

Stollenwerk, T.; O’Gorman, B.; Venturelli, D.; Mandra, S.; Rodionova, O.; Ng, H.; Sridhar, B.; Rieffel, E. G.; and Biswas, R. 2019. Quantum annealing applied to de-conflicting optimal trajectories for air traffic management. *IEEE transactions on intelligent transportation systems*, 21(1): 285–297.

Yamamoto, Y.; Leleu, T.; Ganguli, S.; and Mabuchi, H. 2020. Coherent Ising machines—Quantum optics and neural network Perspectives. *Applied Physics Letters*, 117(16).